 SDHM, vol.3, no.4, pp.211-227, 2007

Electromechanical Admittance – Based Damage Identification Using Box-Behnken Design of Experiments

C.P. Providakis[1] **and M.E. Voutetaki**

Abstract: Piezoceramic transducers have emerged as new tools for the health monitoring of large-scale structures due to their advantages of active sensing, low cost, quick response, availability in different shapes, and simplicity for implementations. In the present paper, a statistical metamodeling utilization of electro-mechanical (E/M) admittance approach by applying piezoelectric materials to the damage identification is investigated. A response surface metamodel is constructed by empirically fitting a model to a set of design points chosen using a Box-Behnken design of experiment (simulation) technique. This empirical fit allows polynomial models to be produced for relating damage parameter such that stiffness reduction to the electromechanical admittance signature generated at piezoelectric sensors at specific frequency ranges. Then, an analytical study based on finite element models is carried out to verify the validity of the present numerical metamodeling technique.

Keyword: Damage identification, Structural health monitoring, Electromechanical admittance, FEM, Box-Behnken design of experiment, Response surface metamodels.

1 Introduction

Engineering structures are often subject to high stress and high load operation condition which may lead to damage and deterioration of their service life. As a result, damage identification is of considerable importance in view of the loss of life and property that may result from structural failure. If damage is detected and identified at early stage then the structure may be economically repaired. Therefore, the need for quick damage detection and identification has necessitated research for the development of many structural heath monitoring techniques.

Many visual or localized experimental damage detection methods have been developed and are routinely employed to a variety of structures [Doherty (1987)]. However, all of these experimental techniques require that the vicinity of the damage be known a priori and that the portion of the structure being inspected is readily accessible. As structures become larger and more complex those techniques become unfeasible and more efficient methods have to be developed. In the aspect of the structural health monitoring using active piezoelectric materials [Leme, Aliabadi, Bezerra and Partridge (2007)], the electromechanical (E/M) admittance (or its inverse impedance) technique is recently used as a promising approach in finding minor changes in structural integrity [Park, Cudney and Inman (2000)], [Park, Sohn, Farrar and Inman (2003)]. The basic concept of this approach is to use high-frequency structural excitations to inspect the local portion of a structure for changes in (E/M) admittance that would indicate imminent damage. The attractive features of the (E/M) admittance technique include its capability of capturing a wide range of structural damage from small to large scale, availability of continuous on-line monitoring, ease of practical application, and cost effectiveness. Implementations of the (E/M) admittance technique have been successfully performed on a number of structures [Lalande, Rogers, Childs and Chaudhry (1996)], [Tseng and Wang (2005)]. However, in these investigations damage is detected by changes in admittance signatures of smart piezoelectric transducers bonded on the structure. The damage identification has so far been restricted to using nonparametric statistical indices to measure changes

[1] Technical University of Crete, Greece

in the admittance signatures. These measures, although effective in detecting the existence of damage, fail to correlate the changes in the admittance signatures to information about the location and severity in order to identify the damage.

Statistical design of experiments (DoE) is the science of obtaining the maximum possible amount of information about a dynamic system with the minimum number of experiments (or simulations) [Goh, 2001]. Computer technology has motivated what used to be a series of complicated mathematical calculations into fairly quick, yet sophisticated, analyses. From this kind of analyses, an expert can optimize process setting design limits in the response. The right design must be chosen in order to fulfill the main objective of the specific problem under investigation. This design is then used to effectively choose an appropriate number of factors that actually control the dynamic system and contribute to its response. Typically, full-factorial or slightly fractional factorial designs are used to identify both main and interaction effects. Finally, when some of the factors have a curvilinear relationship with some of the responses, an optimization stage is then implemented. This optimization uses response surface metamodeling design approaches such as central-composite design (CCD) and Box-Behnken design (BBD) [Anderson and Whitcomb (2004)]. Already, popular in the chemical and industrial engineering communities, response surface metamodeling technique is a statistical method used to 'intelligently' determines which simulation or physical experiments should be run when resources are scarce [Myers and Montgomery (1995)]. The method of response surface metamodeling relies on analysis of variance, or ANOVA, to select a few design points out of the full factorial set that efficiently provide the required information about the full response space. Parametric metamodels may then be fit to these selected design data points using regression methods resulting in a polynomial model that relates input to output parameters.

Although DoE using response surface metamodels is increasingly employed in various fields related to materials science [Harmon (2003)], its application for structural damage detection and identification is not very usual. A review of the limited literature related to the damage detection and identification using the response surface metamodeling technique can be found in the works of County et al [Cundy (2003)], [Cundy, Hemez, Inman and Park (2003)]. They demonstrated that response surface metamodels may be used in structural damage identification problems of two simple dynamic systems. They also showed that metamodels were robust to experimental variability and thus, may be used as reduced order models for both linear and nonlinear structural dynamics systems. In the works of County et al, for the performance of damage identification using response surface metamodels, stiffness and location (as input damage parameters) and natural frequencies (as output features) were chosen and treated as continuous variables due to optimization difficulties encountered using discrete variables. Finally, after the response surface metamodels have been constructed for each output feature, they were then used in an inverse sense to do damage identification.

In the present paper, as a further step, the concept of electro-mechanical admittance-based damage detection technique is integrated with a Box-Behnken design of experiments approach to characterize damage rather merely detecting its presence. The focus of this paper is to demonstrate the feasibility of using a response surface metamodeling technique and Box-Behnken design of experiment (simulation) approaches for identifying damage severity in engineering structures. These approaches use statistically analyzed metamodels developed in the MATLAB statistical toolbox while the required [MATLAB (2006)] inversion problem was solved by using global optimization routines [Henrion and Lasserre (2006)] of polynomials performed in MATLAB environment. The (E/M) admittance (impedance) signatures were numerically resulted from a finite element analysis using COMSOL 3.3a [COMSOL (2006)] commercial software.

2 Electromechanical admittance (EMA) approach

The EMA technique uses piezoelectric materials, such as Lead Zirconate Titanate (PZT), which exhibits the characteristic feature to generate surface charge in response to an applied mechanical stress and conversely, undergo mechanical deformation in response to an applied electric field.

Consider a structural component with a PZT patch bonded on it. The related physical model is shown in Fig. 1 for a square PZT patch of length $2\lambda_{PZT}$ and thickness h_{PZT}.

When a harmonic voltage $V = V_0 e^{j\omega t}$ with $j = \sqrt{-1}$ is applied in the z-direction, producing an electric field $E = E_0 e^{j\omega t}$, an in-plane vibration is induced in both x and y directions. Liang et al [Liang, Sun and Rogers (1994)] first modeled the 1D PZT-structure electro mechanical interaction, while Bhalla & Soh [Bhalla and Soh (2004)] and Soh & Bhalla [Bhalla and Soh (2004)] extended this approach to 2D structures by using the concept of effective impedance. The constitutive equations of the PZT patch are [Bhalla and Soh (2004)]:

$$S_X = \frac{1}{\overline{E}_{PZT}}\left(T_X - \nu_{PZT} T_Y\right) + d_{31}E \tag{1}$$

$$S_Y = \frac{1}{\overline{E}_{PZT}}\left(T_Y - \nu_{PZT} T_X\right) + d_{32}E \tag{2}$$

$$D = \overline{\varepsilon}_{33}E + d_{31}T_X + d_{32}T_Y \tag{3}$$

where S_X and S_Y are strains, T_X and T_Y are stresses, $\overline{E}_{PZT} = E_{PZT}(1 + n \cdot j)$ is the elastic modulus at zero electric field with E_{PZT} being the elastic modulus of the PZT patch, n is the mechanical loss factor, ν_{PZT} is the Poison's ratio, d_{31} and d_{32} are the piezoelectric constants in the x and y directions, respectively, $\overline{\varepsilon}_{33}^T = \varepsilon_{33}^T(1 - \delta \cdot j)$ is the dielectric constant at zero stress with ε_{33} being the dielectric constant of the PZT patch, D is the electric displacement and δ the dielectric loss factor. If the PZT material is isotropic on the x-y plane, which results in $d_{31} = d_{32}$, the electric displacement in equation (3) can be rewritten as:

$$D = \overline{\varepsilon}_{33}^T E + \frac{d_{31}\overline{E}_{PZT}}{1 - \nu_{PZT}}(u' + v' - 2d_{31}E)$$

where $()' = \vartheta()/\vartheta x$ and u, v are the displacements responses in x and y direction , respectively which can be derived as the solution of the in-plane vibration problem of the PZT patch [Zhou, Liang and Rogers (1995)], [Bhalla and Soh (2003)]:

$$\rho_{PZT}\ddot{u} = \frac{\overline{E}_{PZT}}{1 - \nu_{PZT}^2}u'' \tag{4}$$

$$\rho_{PZT}\ddot{v} = \frac{\overline{E}_{PZT}}{1 - \nu_{PZT}^2}v'' \tag{5}$$

where $(\ddot{x}) = \vartheta^2(x)/\vartheta t^2$ and ρ_{PZT} is the density of the PZT patch. The electric current passing through the PZT patch, can be considered to be given by

$$I = j\omega \int_{-\frac{\ell_{PZT}}{2}}^{\frac{\ell_{PZT}}{2}} \int_{-\frac{\ell_{PZT}}{2}}^{\frac{\ell_{PZT}}{2}} D\,dx\,dy \tag{6}$$

Considering that the electric field is defined by

$$E = \frac{V}{h_{PZT}} \tag{7}$$

and that the input voltage V is an AC voltage of 1 Volt (rms) in magnitude, the electric admittance of the PZT patch can be expressed as:

$$Y = \frac{I}{V} = j\,\omega\,\Sigma Q_i \tag{8}$$

where ΣQ_i is the total charge over the whole surface of the PZT patch.

3 Response surface methodology (RSM)

The conventional methodology of changing one variable at a time and investigating the effect of the variable on the response is a complicated technique, particularly in a multivariable system or if more than one response are of importance. Designs of experiments (simulations) are statistical methodologies which may be used for optimizing such multivariable systems. Many statistical experimental designs have been recognized as useful techniques to optimize the process variables. Response surface methodology (RSM) is

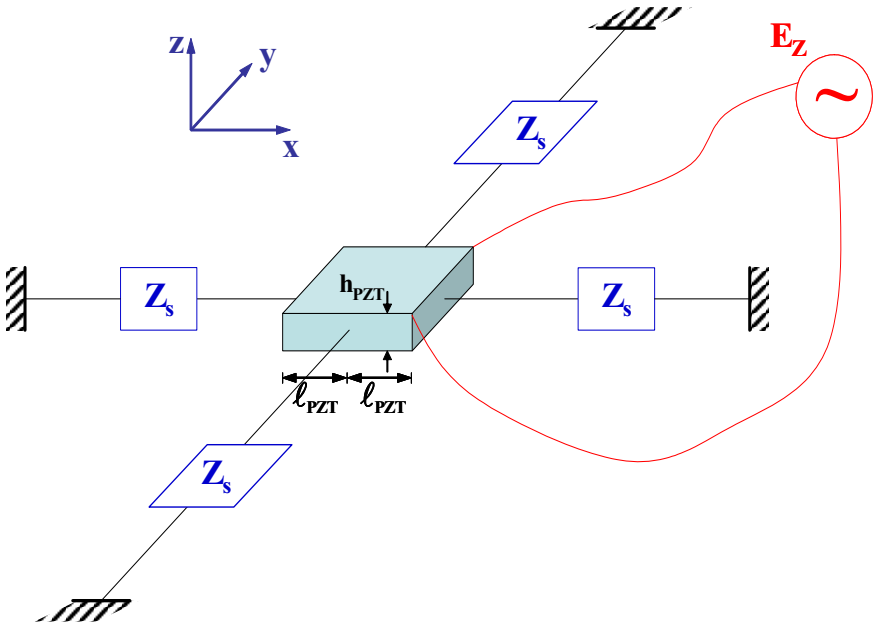

Figure 1: Model of interaction between PZT and structure

used when only a few significant factors are involved in the optimization without the use the need for studying all possible combinations experimentally. Further, the input levels of the different variables for a particular level of response may also be determined.

RSM comprises a set of statistical methodologies for model building and model exploitation. By careful design and analysis of experiments (simulations), it seeks to relate a response or output variable to the levels of a number of predictors of input variables that affects it. It allows calculations to be made of the response at intermediate levels which were not experimentally investigated and show the direction in which to move if we wish to change the input levels so as to decrease or increase the response.

The design procedure of RSM is as follows [Charles and Kenneth (1999)], [Box, Hunter and Hunter (1978)]:

- Designing of a series of experiment (simulation) for adequate and reliable measurement of the response of interest.
- Developing a polynomial metamodel of the second order response surface with the best fittings.
- Finding the optimal set of experimental parameters that produce a maximum or minimum value of response.
- Representing the direct and interactive effects of process parameters through two or three dimensional plots.

If all variables are assumed to be measurable, the response surface can be expressed as follows:

$$Y = f(X_1, X_2, X_3, \ldots, X_k) \tag{9}$$

where Y is the response (output) of the system, and X_i the variables of the action called factors (input).

The objective is to optimize the response variable y. It is assumed that the independent variables are continuous and controllable by experiments (simulations) with negligible errors. It is required to find a suitable approximation for the true functional relationship between independent variables and the response surface. Usually a second-order metamodel is utilized in response surface methodology:

$$Y = b_0 + \sum_{i=1}^{k} b_i X_i + \sum_{i=1}^{k} b_{ii} X_i^2 + \sum_{i=1}^{k-1} \sum_{j=2}^{k} b_{ij} X_i X_j + \varepsilon \tag{10}$$

Where X_1, X_2, X_3, ..., X_k are the input factors which influence the response Y; b_0, b_{ii} ($i = 1,2,\ldots,k$), b_{ij} ($i = 1,2,\ldots,k$; $j = 1,2,\ldots,k$) are unknown parameters and ε is a random error. The b coefficients, which could be determined in the second-order metamodel, are obtained by the least square method. In general eq. (10) can be written in matrix form

$$Y = bX + \varepsilon \tag{11}$$

where Y is defined to be a matrix of the measured values of the response, X to be a matrix of the input independent variables. The matrices b and ε consist of coefficients and errors, respectively. The solution of Eq. (11) can be obtained by the matrix approach

$$b = (X'X)^{-1}X'Y \tag{12}$$

where X' is the transpose of the matrix X and $(XX')^{-1}$ is the inverse of the matrix $X'X$. The number of input parameters of the second-order polynomial may be unlimited. If more input parameter levels are included in a model, then a higher order metamodel may be constructed. The more levels incorporated into a design, the larger the design will be for the same resolution of a design with fewer input parameter levels. When performing response surface analysis, it is customary to use normalized or "coded" input parameter values between the values -1 and +1, in order to give a better idea of the relative importance of each of the parameter. The three usual natural values of the input parameters, X_i, (corresponding to low, midrange/center point, and high values) are mapped into three coded levels, x_i, corresponding to -1, 0, and +1, respectively. In general, the relationship between the natural and the coded input parameter value may be expressed as

$$x_i = \frac{2 \cdot X_i - (X_i^{MAX} + X_i^{MIN})}{(X_i^{MAX} - X_i^{MIN})} \tag{13}$$

where X_i^{MAX} and X_i^{MIN} correspond to the low- and high-natural values of the ith independent input parameter.

Different types of RSM designs include 3-level factorial design, central composite design (CCD), Box-Behnken design, and D-optimal design. A modified central composite experimental design, Box-Behnken design, is an independent, rotatable or nearly rotatable quadratic design (contains no embedded factorial or fractional factorial design), in which the treatment combinations are at the midpoints of the edges of the process space and at the center. Box-Behnken design requires an experiment (simulation) number according to N=k2+k+cp, where (k) is the number of the factors (input parameters), and (cp) is the replicate number of the central design point [Souza, Walter and Ferreira (2005)]. Box-Behnken is a spherical, revolving design. Viewed as a cube (Fig. 2a), it consists of a central point and the middle points of the edges. However, it can also be viewed as consisting of three interlocking 2^2 factorial design and a central point (Fig 2b) [Massart, Vandeginste, Buydens, Jong, Lewi and Smeyers (2003)]. It has been applied for optimization of several chemical and physical processes [Box and Behnken (1960)], [Montgomery (2001)].

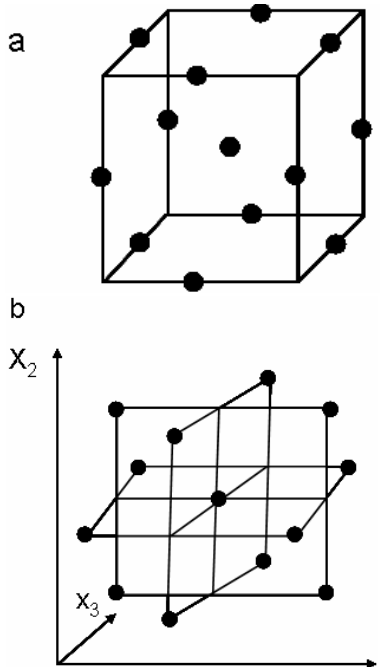

Figure 2: Box-Behnken design (three level model)

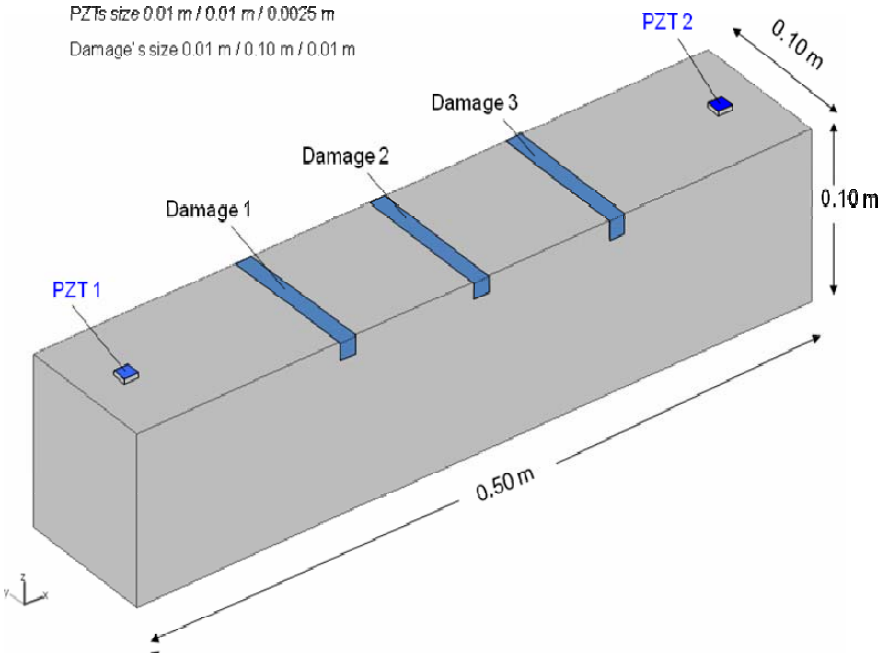

Figure 3: Three-dimensional beam sample model

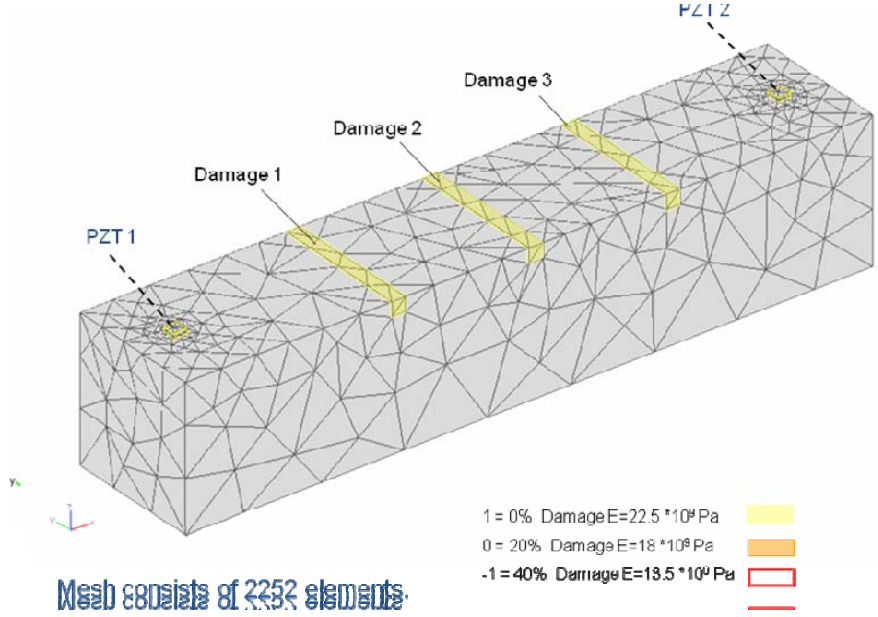

Figure 4: Three-dimensional finite element beam sample model

4 Box-Behneken experiment (simulation)

4.1 Methodology

Since in real engineering applications, it would be impractical or even, in some times, impossible to actually produce a great number of damaged structures in order to be used for training metamodels, computer simulations rather than experimental in situ investigations will be used here to built response surface models to perform the present damage identification. The system of interest is a concrete beam (beam dimensions 0.1 m by 0.1 m by 0.5 m) with three pre-selected locations of the upper surface at which three differ-

ent designed levels of damage are considered. In the present investigation, reduced stiffness coefficients constitute "damage" to the system. The healthy system was defined as having a stiffness coefficient of $E = 22.5 \times 10^9$ N/m for the whole beam. Damage was defined as percentage of stiffness coefficient E distributed in cross-width 3D regions (region dimensions, 0.01 m in depth by 0.01m in thickness) located at three pre-selected distances D_1=150 mm, D_2=250 mm and D_3=350 mm, respectively, from the left end of the beam as shown in Fig. 3.

Our primary goal of the present study is to develop response surface metamodels that isolate the effect of the three damage configuration parameters (3-factor experiment) (e.g., Damage1 at location D_1, X_1; Damage2 at location D_2, X_2; Damage3 at location D_3, X_3) on the electromechanical admittance signal recorded (simulated) at the surfaces of PZTs. Three different damage levels (3-level experiment) at D_1 location (X_1=0%, 20%, and 40%), at D_2 location (X_2=0%, 20%, and 40%) and at D_3 location (X_3=0%, 20%, and 40%) were considered in this study. In order to perform the electromechanical admittance approach the concrete beam is excited using two piezoceramic 3-D patches (PZTs dimensions, 0.01 m by 0.01 m by 0.0025 m) each located at a distance of 25 mm from the ends of the beam as shown in Fig. 3.

The analysis was performed using the commercial finite element software COMSOL 3.3a [COMSOL (2006)]. The model used 2252 finite elements. The damages were represented as colored meshed regions at the upper surface of the sample beam model in the Fig. 4. Frequency response analysis was performed using zero vertical displacement boundary conditions at the lower surface of the beam.

Basically, the electromechanical admittance approach consists in obtaining the frequency response of the real part of electromechanical admittance of each PZT patch, using frequencies higher than 30 kHz, in order to further compare the modification of these signals as caused by the damage. A modification in these signals would indicate the presence of damage [Park, Sohn, Farrar and Inman (2003)]. In this study, to determine the most sensitive frequency band to be monitored for the investigated concrete beam sample, a trial and error procedure is adopted. By observing the peaks of the real part of the electromechanical admittance signals as obtained at piezoelectric patches - PZT_1 and PZT_2 – it become evident that a frequency band between 30-40 kHz is the most adequate frequency band test configuration. Plots of the real part of the electromechanical admittance for the selected band between 30-40 kHz for PZT_1 and PZT_2 patches can be shown in Fig. 5 and Fig. 6.

Then, the real part of the electromechanical admittance values at six selected frequencies (f_1=30 kHz, f_2=32 KHz, f_3=34 kHz, f_4=36 kHz, f_5=38 kHz and f_6=40 kHz) for both PZT patch (PZT_1 and PZT_2), in the investigated frequency band, are considered as output features. The number of output features used in the present approach is crucial, since the more output features incorporated into the design, the larger the design will be for the same resolution of a design with fewer output features.

4.2 Box-Behnken results and discussion

Among all the RSM designs, in this study, the Box-Behnken design was specifically selected since it requires fewer runs (15 runs) in a 3-factor experimental design. A 3-factor, 3-level design is suitable for exploring quadratic response surfaces and constructing second order polynomials. This cubic design is characterized by set of points lying at the midpoint of each edge of a multidimensional cube and center point replicates (n=3) whereas the "missing corners" help the experiment (simulation) to avoid the combined factor extremes. This property prevents a potential loss of data in those cases. The special arrangement of the Box-Behnken design levels allows the number of design points to increase at the same rate as the number of metamodel polynomial coefficients b of the second-order equation (10). For three factors, for example, the design can be constructed as three blocks of four experiments consisting of a full two-factor factorial design with the level of the third factor set at zero [Souza, Walter and Fer-

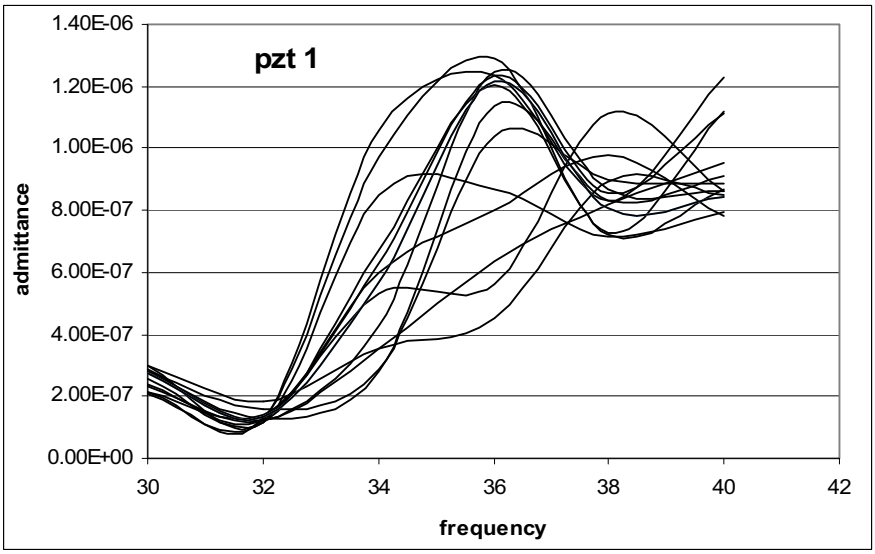

Figure 5: Frequency response of real part of the electromechanical admittance between 30-40 kHz frequency band at PZT_1 surfaces

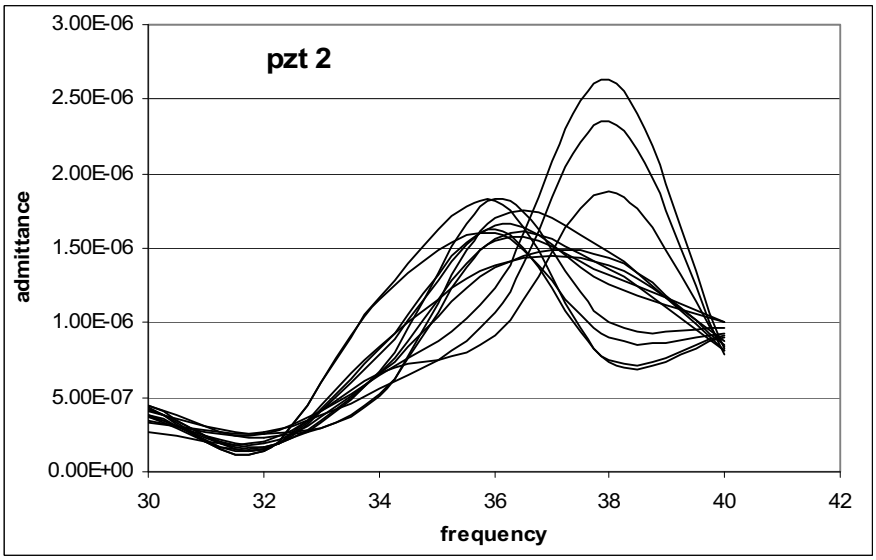

Figure 6: Frequency response of real part of the electromechanical admittance between 30-40 kHz frequency band at PZT_2 surfaces.

reira (2005)].

Tab. 1 summarizes the natural values and coded values of the (3-factor, k=3) independent input variables (X_1, X_2, X_3) considered in this study.

Defining the real part of the simulated electromechanical admittance signal obtained at the l-th PZT patch of the finite element model and at the m-th pre-selected frequency of the simulated signal as the predicted response quantity,Y_l^m, equation 10 may be expressed in expanded form

$$Y_l^m = b_0 + b_1x_1 + b_2x_2 + b_3x_3 + b_{11}x_1^2 + b_{22}x_2^2 + b_{33}x_3^2 + b_{12}x_1x_2 + b_{13}x_1x_3 + b_{23}x_2x_3 \quad (14)$$

where x_i is the coded level of the i^{th} independent variable (factor) $(i = 1, 2, 3)$.

Consistent with reference [Box and Behnken (1960)], the experimental (simulation) matrix used in the present investigation to solve for the

Table 1: Natural and coded values of the input parameters.

i	Damage variable	Natural value, X_i	Coded value, X_i
1	At location D1=	0%	-1
		20%	0
		40%	+1
2	At location D2=	0%	-1
		20%	0
		40%	+1
3	At location D3=	0%	-1
		20%	0
		40%	+1

regression coefficients (b_0, b_i, and b_{ij}; $i, j = 1,2,3$) required that the high- and low-coded levels of any two independent factors be paired in all possible combinations while fixing the third independent factor at its coded midrange level value. These runs are performed in combination with three additional runs in which the independent factors are fixed at their midrange level values (x_1=x_2=x_3=0), resulting in a total of 15 runs. The latter three runs are important for assessing the degree of curvature in the response as well as for evaluating the model error and goodness of fit. Tab. 2 and 3 show the test matrix used in this study in terms of the coded levels of the independent factors as well as the real part of the electromechanical admittance Y_1^m and Y_2^m of the m-th pre-selected frequency simulated at the electrical surfaces of PZT_1 and PZT_2 patches, respectively.

The regression coefficients were selected such that the error ε between the predicted values of the real part of the electromechanical admittance, and the corresponded finite element simulated values, Y_l^m, is minimized through a least square estimation methodology performed in the Statistical Toolbox of MATLAB [MATLAB (2006)]. Thus, using equation 12, in combination with the simulated values of electromechanical admittance from Tables 2 and 3, the quadratic response surfaces characterizing the real part of the electromechanical admittances may be expressed as in equation 14 by using the regression coefficients b shown in Tables 4 and 5. The coefficients b are presented in those Tables as a function of the six pre-selected frequencies ($1^{st} \ldots 6^{th}$) for the first PZT patch (PZT_1) and the six frequencies ($7^{th} \ldots 12^{th}$) for the second PZT patch (PZT_2).

Below, in Fig. 7 and Fig. 8, presented two examples of the response surfaces generated, at PZT locations PZT_1 and PZT_2, respectively, in terms of two of the three input damage parameters $D_1(x_1)$, $D_2(x_2)$ and $D_3(x_3)$ while the third input damage parameter is kept fixed.

4.3 Damage identification inverse problem

At the final stage of the present damage identification methodology, after the response surface metamodels have been constructed on the set of Box-Behnken design points they should be used in an inverse sense to do damage identification. The problem : "Knowing the output values of the real part of the electromechanical admittance at specific PZT patch locations, what were the input damage level parameters at specific locations that may lead to such values ?" must be analyzed and solved accordingly.

This problem was first attempted using a simple error minimization scheme performing the MATLAB *fminsearch* routine [MATLAB (2006)]. This simple optimization scheme stopped once a minimum between the actual and the predicted output feature value of the real part of the electromechanical admittance was achieved. But, it was very easy to prove that these minimum values were not unique since this kind of inverse problems has many local minima. Thus, the advanced MATLAB routine *Gloptipoly* (www.laas.fr/∼henrion/software/gloptipoly) [Henrion and Lassere (2006)] has been used to solve the global optimization problem of the multivariable present work. It may generate a series of lower bounds monotonically converging to the global optimum at low computational cost.

To test how well the global optimization procedure through *Gloptipoly* routine worked, a set of runs was used which includes 15 Box-Behnken design points plus 7 points not included in the design, for a total of 22 points. That is, knowing the twelve output feature values (2 PZT locations x 6 pre-selected frequencies) of real part of the

Table 2: Box-Behnken test matrix for PZT_1 surfaces

Run k	Damage x_1	Damage x_2	Damage x_3	Y_1 at 30kHz	Y_1 at 32kHz	Y_1 at 34kHz	Y_1 at 36kHz	Y_1 at 38kHz	Y_1 at 40kHz
1	-1	-1	0	2.107E-07	1.218E-07	1.073E-06	1.242E-06	8.529E-07	1.279E-06
2	-1	1	0	2.358E-07	1.384E-07	8.809E-07	1.331E-06	6.871E-07	9.708E-07
3	1	-1	0	2.589E-07	1.340E-07	5.003E-07	1.238E-06	8.550E-07	9.776E-07
4	1	1	0	2.644E-07	1.251E-07	4.342E-07	1.195E-06	8.426E-07	8.243E-07
5	-1	0	-1	2.100E-07	1.238E-07	1.018E-06	1.272E-06	7.803E-07	1.198E-06
6	-1	0	1	2.463E-07	1.380E-07	9.709E-07	1.239E-06	7.383E-07	1.005E-06
7	1	0	-1	2.560E-07	1.360E-07	4.804E-07	1.280E-06	7.990E-07	9.547E-07
8	1	0	1	2.786E-07	1.319E-07	4.774E-07	1.058E-06	8.810E-07	7.995E-07
9	0	-1	-1	2.260E-07	1.230E-07	7.800E-07	1.236E-06	8.926E-07	1.188E-06
10	0	-1	1	2.544E-07	1.391E-07	7.649E-07	1.193E-06	8.718E-07	9.975E-07
11	0	1	-1	2.410E-07	1.412E-07	6.558E-07	1.332E-06	7.484E-07	9.409E-07
12	0	1	1	2.783E-07	1.236E-07	6.266E-07	1.112E-06	7.755E-07	8.060E-07
13	0	0	0	2.447E-07	1.394E-07	7.317E-07	1.287E-06	7.914E-07	1.003E-06
14	0	0	0	2.447E-07	1.394E-07	7.317E-07	1.287E-06	7.914E-07	1.003E-06
15	0	0	0	2.447E-07	1.394E-07	7.317E-07	1.287E-06	7.914E-07	1.003E-06

Table 3: Box-Behnken test matrix for PZT_2 surfaces

Run k	Damage x_1	Damage x_2	Damage x_3	Y_1 at 30kHz	Y_1 at 32kHz	Y_1 at 34kHz	Y_1 at 36kHz	Y_1 at 38kHz	Y_1 at 40kHz
1	-1	-1	0	4.247E-07	1.326E-07	1.219E-06	1.727E-06	7.797E-07	9.044E-07
2	-1	1	0	4.234E-07	1.431E-07	1.004E-06	1.818E-06	8.785E-07	9.766E-07
3	1	-1	0	4.523E-07	1.646E-07	6.504E-07	1.831E-06	8.005E-07	8.970E-07
4	1	1	0	4.071E-07	1.808E-07	5.940E-07	1.690E-06	1.210E-06	9.605E-07
5	-1	0	-1	4.165E-07	1.348E-07	1.210E-06	1.599E-06	9.055E-07	9.137E-07
6	-1	0	1	4.313E-07	1.411E-07	1.020E-06	1.915E-06	8.285E-07	9.234E-07
7	1	0	-1	4.537E-07	1.624E-07	6.459E-07	1.708E-06	8.216E-07	9.135E-07
8	1	0	1	3.990E-07	1.895E-07	5.859E-07	1.696E-06	1.257E-06	9.187E-07
9	0	-1	-1	4.326E-07	1.394E-07	9.752E-07	1.602E-06	7.803E-07	9.163E-07
10	0	-1	1	4.376E-07	1.502E-07	8.377E-07	1.910E-06	7.697E-07	9.019E-07
11	0	1	-1	4.297E-07	1.506E-07	8.208E-07	1.697E-06	8.641E-07	9.693E-07
12	0	1	1	3.950E-07	1.626E-07	7.064E-07	1.693E-06	1.195E-06	9.696E-07
13	0	0	0	4.386E-07	1.484E-07	8.416E-07	1.820E-06	7.849E-07	9.367E-07
14	0	0	0	4.386E-07	1.484E-07	8.416E-07	1.820E-06	7.849E-07	9.367E-07
15	0	0	0	4.386E-07	1.484E-07	8.416E-07	1.820E-06	7.849E-07	9.367E-07

Table 4: Coefficients of Equation 14 for PZT_1

Equation / Coefficient	1^{st}	2^{nd}	3^{rd}	4^{th}	5^{th}	6^{th}
b_o	2.447E-07	1.394E-07	7.317E-07	1.287E-06	7.914E-07	1.003E-06
b_1	1.937E-08	6.201E-10	-2.563E-07	-3.896E-08	3.986E-08	-1.120E-07
b_2	8.690E-09	1.292E-09	-6.511E-08	7.825E-09	-5.234E-08	-1.124E-07
b_3	1.555E-08	1.072E-09	-1.181E-08	-6.466E-08	5.782E-09	-8.423E-08
b_{11}	-4.896E-09	-6.370E-09	3.148E-08	-3.297E-08	3.833E-08	3.870E-08
b_{22}	-3.435E-09	-4.566E-09	1.105E-08	-4.704E-08	3.099E-08	9.543E-09
b_{33}	2.243E-09	-8.422E-09	-3.530E-09	-4.402E-08	1.197E-08	1.381E-08
b_{12}	-2.216E-09	-4.443E-09	1.014E-08	-2.085E-08	-2.251E-09	7.993E-09
b_{13}	-4.115E-11	-5.146E-09	-1.976E-08	-1.516E-08	2.020E-08	1.765E-09
b_{23}	5.257E-09	-2.564E-09	-5.169E-09	-5.415E-08	1.045E-08	-2.186E-08

Table 5: Coefficients of Equation 14 for PZT_2

Equation / Coefficient	7^{th}	8^{th}	9^{th}	10^{th}	11^{th}	12^{th}
b_o	4.386E-07	1.484E-07	8.416E-07	1.820E-06	7.849E-07	9.367E-07
b_1	2.024E-09	1.821E-08	-2.471E-07	-1.669E-08	8.715E-08	-3.546E-09
b_2	-1.149E-08	6.283E-09	-6.958E-08	-2.150E-08	1.272E-07	3.207E-08
b_3	-8.713E-09	7.025E-09	-6.275E-08	7.601E-08	8.489E-08	8.793E-11
b_{11}	-1.099E-08	1.423E-09	3.951E-08	-5.789E-08	7.770E-08	-2.181E-09
b_{22}	-1.737E-08	5.204E-09	3.251E-08	-8.187E-08	1.281E-07	-1.143E-09
b_{33}	-9.926E-09	2.850E-10	5.770E-09	-7.799E-08	8.544E-08	3.698E-09
b_{12}	-5.160E-09	6.552E-09	2.782E-08	-2.493E-08	9.157E-08	-1.201E-08
b_{13}	-6.530E-09	3.160E-10	-2.531E-09	-2.880E-08	4.072E-08	9.947E-09
b_{23}	-8.294E-09	1.968E-09	-4.035E-09	-6.589E-08	7.670E-08	-7.358E-09

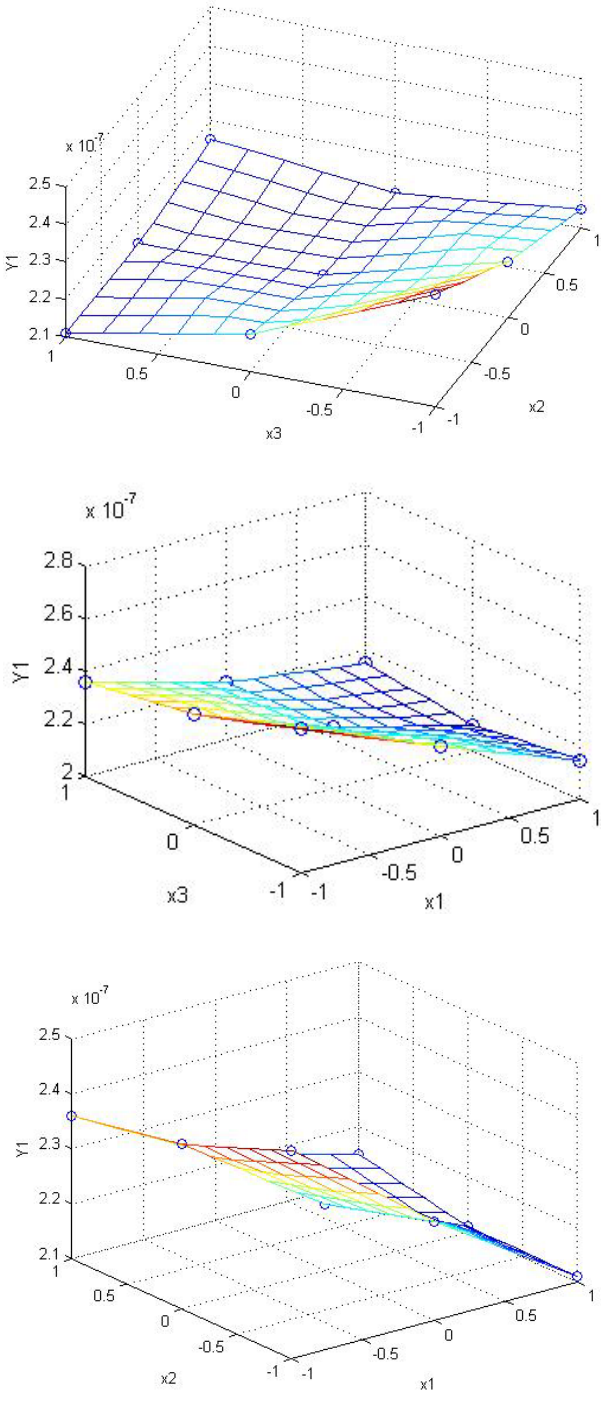

Figure 7: RSM 3D-plots at PZT_1 surfaces

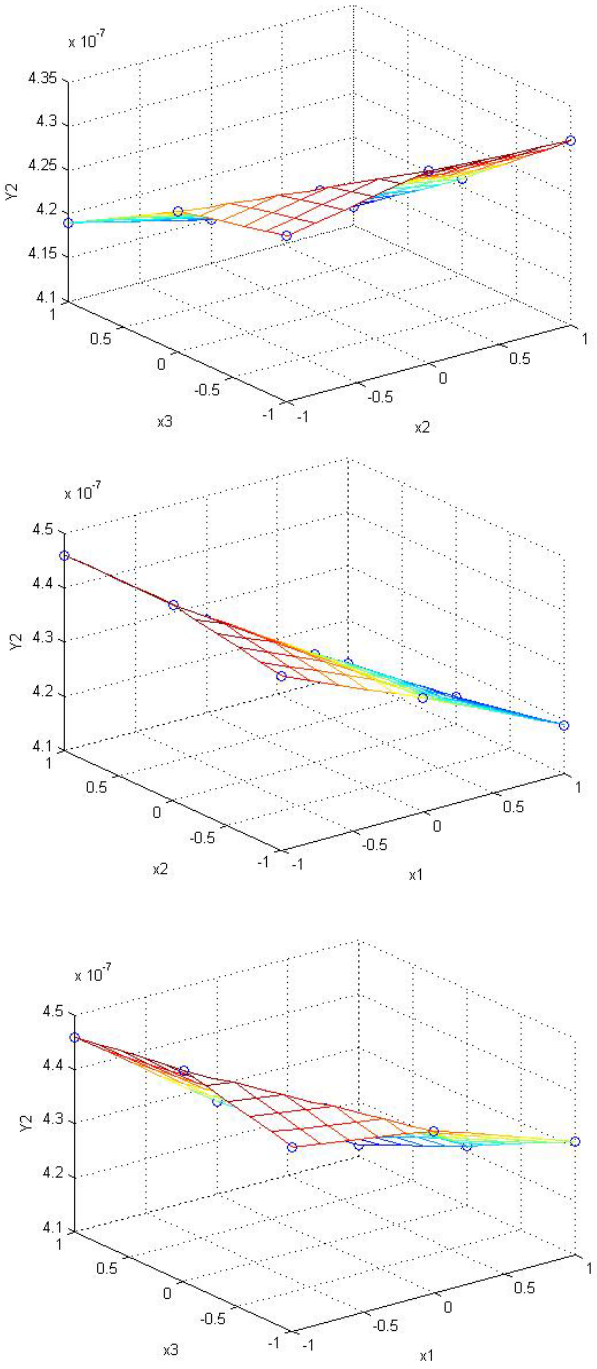

Figure 8: RSM 3D-plots at PZT_2 surfaces

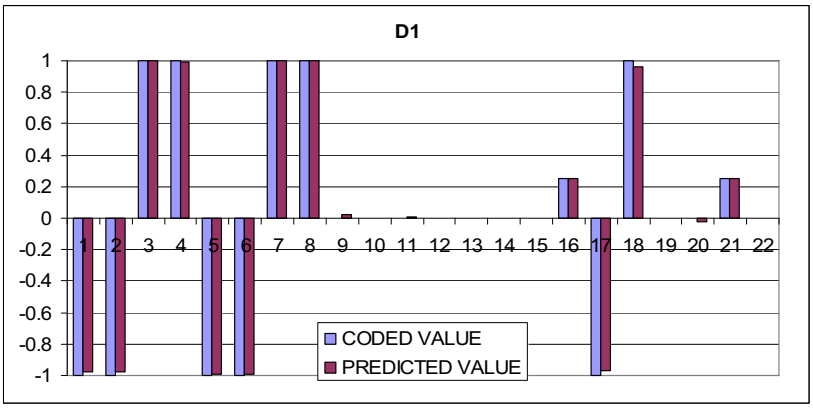

Figure 9: Comparison between actual and predicted coded value for Damage 1

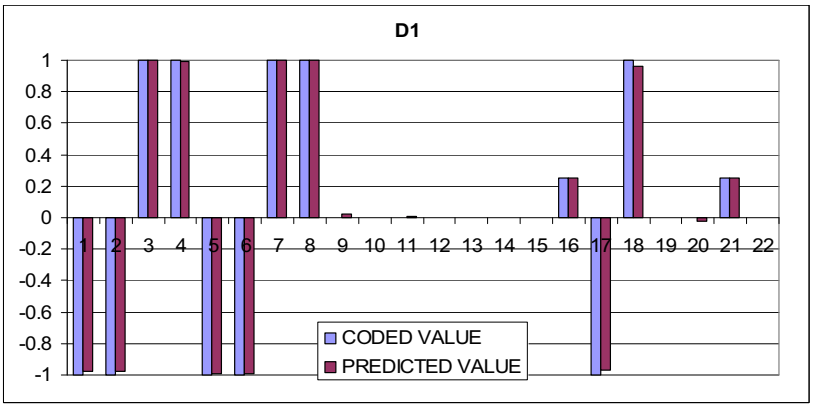

Figure 10: Comparison between actual and predicted coded value for Damage 2

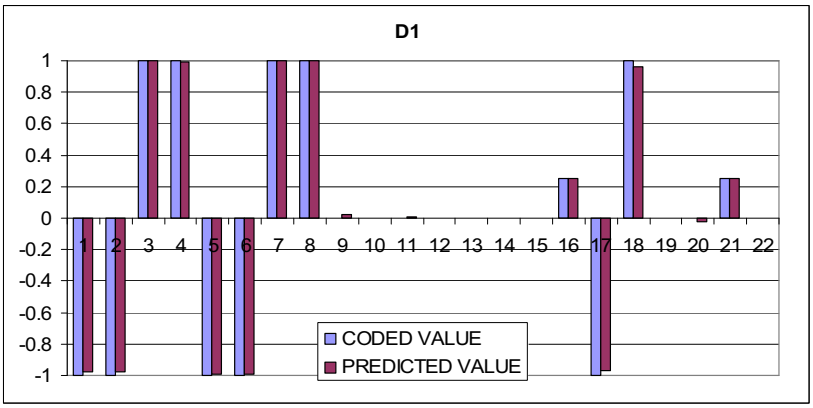

Figure 11: Comparison between actual and predicted coded value for Damage 3

Table 6: Set of damage identification results. Box-Behnken design points are shown in bolds

	Damage parameters			Predicted damage parameters by *Gloptipoly*		
Run	X_1	X_2	X_3	X_1	X_2	X_3
1	-1	-1	0	-0.98	-0.94	0.32
2	-1	1	0	-0.98	1	0.22
3	1	-1	0	1	-0.91	0.05
4	1	1	0	0.99	0.37	0.03
5	-1	0	-1	-0.99	0.023	-0.64
6	-1	0	1	-0.99	0.01	1.03
7	1	0	-1	1	0.056	-0.94
8	1	0	1	1	0.05	0.89
9	0	-1	-1	0.02	-0.87	-0.36
10	0	-1	1	0	-0.9	1
11	0	1	-1	0.01	1.1	-0.91
12	0	1	1	0	1	0.93
13	0	0	0	0	0.023	0.09
14	0	0	0	0	0.023	0.09
15	0	0	0	0	0.023	0.09
16	0.25	-0.5	1	0.25	-0.44	1
17	-1	1	-1	-0.97	1	-0.87
18	1	-1	1	0.96	-0.82	1
19	0	0.5	0	0	0.5	0.12
20	0	-0.5	0	-0.02	-0.26	0
21	0.25	0.25	0.75	0.25	0.28	0.86
22	0	0.25	0	0	0.33	0.2

electro-mechanical admittance, could the damage input parameter level value at the locations D_1, D_2 and D_3 be identified. The damage identification results are shown in Table 6, with the damage level to be predicted by the *Gloptipoly* optimization routine.

Results are also shown in Fig. 9, Fig. 10 and Fig. 11, in the form of three plots of actual damage level versus predicted damage level from the global optimization procedure of *Gloptipoly* routine.

It can be observed that damage predictions are much more successful at locations D_1 and D_3. This is an expected result since it is well known that locations closer to the PZT sensor locations are predicted better than locations far away from them. It can be also seen in these figures that the present inverse formulation captures better the main trend for the predicted damage level in the simulated Box-Behnken design points than the points that are not in the design set. One possible reason for higher damage identification error might be because continuous input damage variables were used to represent discrete damage parameters.

5 Conclusions

With the combination of finite element method and Box-Behnken design of experiment, analysis of damage parameters effect was greatly simplified and the process of damage identification was made efficient. Having appropriate quadratic response surface metamodels of the input parameter variations is important in analyzing a structure's current state of health and predicting structural behaviour in various conditions. The health monitoring process proposed here that capitalizes the feature training of appropriate design points in

the response surface metamodeling technique for the minimization of the associated prediction error can be efficiently used in determining the damage state of a structure. Using this features the magnitude of the damage (altered stiffness) was correctly identify for nearly 70% of the simulations tested. Stiffness reduction identification was performed by solving an inverse problem using a set of twelve quadratic response surface polynomials which were trained on 15 Box-Behnken design points. Results for all sets of simulations were encouraging with correct trends captured for number of damage locations.

6 Reference

Adams, D.E. (2001): Frequency domain ARX models and multi-harmonic FRF estimators for nonlinear dynamic systems, *Journal of Sound and Vibrations*, vol. 250, pp. 935-950.

Anderson, M.; Whitcomb, P. (2004): *RSM Simplified, Optimizing Processes Using Response Surface Methods for Design of Experiments*, NY: Productivity Press.

Ayres, J.W.; Lalande, F.; Chaudhry, Z.; Rogers, C.A. (1998): Qualitative impedance-based health monitoring of civil infrastructures, *Smart Materials and Structures*, vol. 7, pp. 599-605.

Bhalla, S.; Soh, C.K. (2003): Structural Impedance Damage Diagnosis by Piezo-transducers, *Journal of Earthquake Engineering Structures and Dynamics*, vol.32, 2003, pp. 1897-1916.

Bhalla, S.; Soh, C.K. (2004a): Health Monitoring by Piezo-impedance Transducers I: modelling, *Journal of Aerospace Engineering, ASCE*, vol.17, pp. 154-165.

Bhalla, S.; Soh, C.K. (2004b): Structural Health Monitoring by Piezo-impedance Transducers I: modelling, *Journal of Aerospace Engineering, ASCE*, vol.17, pp. 154-165.

Box E.P.; Benhken D.W. (1960): *Technometrics 2* (1960), pp. 195.

Box G.E.P.; Hunter W.G.; Hunter J.S. (1978): Statistics for experiments—-an introduction to design, data analysis and model building. John Wiley & Sons, New York.

Castillo, E. (1998): Extreme Value Theory in Engineering, *Academic press Series in Statistical Modeling and Decision Science*, Academic press, san Diego, CA.

Charles, R.H.; Kennneth, V.T. (1999): *Fundamental concepts in the design of experiments*, University Press, Oxford.

COMSOL (2005): Ltd, London, Comsol Multiphysics Modelling 3.3, www.comsol.com, 2005, Users Guide.

Cundy, A.L.; Hemez F.M.; Inman D.J.; Park G. (2003): Use of response surface metamodels for damage identification of a simple non-linear system, *Key Engineering Materials*, vols. 245-246, pp. 167-174.

Cundy, A.L. (2002): Use of Response Surface Metamodels in Damage Identification of Dynamic Structures Masters Thesis, Virginia Polytechnic Institute and State University.

Doherty, J.E. (1987): Handbook of Experimental Mechanics, Chapt. 12, *Society for experimental Mechanics*, Inc, Bethel, CT, USA.

Giurgiutiu, V.; Zagrai, A.N. (2002): Characterization of Piezoelectric Wafer Active Sensors, *Journal of Vibration Acoustics, ASME*, vol.124, pp. 116-125.

Goh, T.N. (2001): Pragmatic Approach to Experimental Design in Industry, *Journal of Applied Statistics*, vol.28, pp. 391-398.

Henrion, D.; Lasserre, J. (2003): GloptiPoly: Global optimization over polynomials with Matlab and SeDuMi, *ACM Trans. Math. Soft.*, 29: 165-194.

Henrion, D.; Lasserre, J.B. (2006): Gloptipoly: Global optimization over polynomials with Matlab and Se-DuMi by Didier Henrion and Jean Lasserre. Available at http://www.laas.fr/_henrion/software/gloptipoly/, versi-on 2.3.0 of December 13 2006.

Koh, Y.L.; Rajic, N.; Chiu, W.K.; Galea, S. (1999): Smart structures for composite repair, *Composite Structures*, vol. 47, pp. 745-752.

Lalande, F.; Rogers, C.A.; Childs, B.;

Chaudhry, Z. (1996): High frequency impedance analysis for NDE of complex precision parts, *Proceedings of the SPIE Conference on Smart Structures and Materials, Bellingham*, Washington, vol. 2717, pp. 237-245.

Leme, S.P.L.; Aliabadi, M.H.; Bezerra, L.M.; Partridge, P.W. (2007): An investigation into active strain transfer analysis in a piezoelectric sensor system for structural health monitoring using the dual boundary element method, *Structural Durability and Health Monitoring*, vol. 3(3), pp. 121-132.

Liang, C.; Sun, F.P; Rogers, C.A. (1994): Coupled Electro-mechanical Analysis of Adaptive Material Systems Determination of the Actuator Power Consumption and System Energy Transfer, *Journal of Intelligent Materials Systems and Structures*, vol.5, pp. 15-20.

Massart, D.L.; Vandeginste B.G.M.; Buydens L.M.C.; Jong S.D.; Lewi P.J.; Smeyers J.V. (2003): *Handbook of chemometrics and qualimetrics Part A*, Elsevier, Amsterdam.

MATLAB, The Mathworks Inc. U.S. (2006): www.mathworks.com., 2006, Users Guide.

Myers, R.H.; Montgomery, D.C. (1995): *Response Surface Methodology*, John Wiley and Sons, Inc., New York, NY.

Park, G.; Cudney, H.H.; Inman, D.J. (2001): Feasibility of using Impedance-based Damage Assessment for Pipeline Structures, *Journal of Earthquake Engineering Structures and Dynamics*, vol.30, pp. 1463-1474.

Park, G.; Cudney, H.H.; Inman, D.J. (2000): Impedance-based health monitoring of civil structural components, *Journal of Infrastructures Systems*, vol. 6, pp. 153-160.

Park, G.; Rutherford, A.; Sohn, H.; Farrar, C.R. (2005): An outlier analysis framework for impedance-based structural health monitoring, *Journal of Sound and Vibrations*, vol. 286, pp. 229-250.

Park, G.; Sohn, H.; Farrar C.R.; Inman, D.J. (2003): Overview of piezoelectric impedance based health monitoring and path forward, *Journal of Shock and Vibration Digest*, vol. 35(6), pp.451–463.

Park, G.; Sohn, H.; farrar, C.R.; Inman, D.J. (2003): Overview of piezoelectric impedance-based health monitoring and path forward, *The Shock and Vibration Digest*, vol. 35, pp. 451-463.

Soh, C.K.; Tseng, K.K.H.; Bhalla, S.; Gupta, A. (2000): Performance of Smart Piezoceramic Patches in Health Monitoring of a RC Bridge, *Journal of Smart Materials and Structures*, vol. 9, pp. 533-542.

Sohn, H.; Allen, D.W.; Worden, K.; Farrar, C.R. (2005): Structural damage classification using extreme value statistics, *Journal of Dynamic Systems Measurements and Control ASME*, vol. 127, pp. 125-132.

Souza, A. S.; Walter, N.L.; dos Santos; Sérgio Ferreira, L.C. (2005): Application of Box–Behnken design in the optimization of an on-line pre-concentration system using knotted reactor for cadmium determination by flame atomic absorption spectrometry, *Spectrochimica*, Acta Part B 609, pp. 737-742.

Tseng, K.K.; Naidu, A.S.K. (2002): Non-parametric damage detection and characterization using smart piezoelectric material, *Smart Materials and Structures*, vol.11, pp. 317-329.

Tseng, K.K.; Wang, L. (2005): Impedance-based method for nondestructive damage identification, *Journal of Engineering Mechanics*, vol.131, pp. 58-64.

Winston, H.A.; Sun, F.; Annigeri, B.S. (2001): Structural health monitoring with piezoelectric active sensors, Transactions of the ASME — *Journal of Engineering for Gas Turbine and Powe*r, 123(2): 353-358.

Zagrai, A.N.; Giurgiutiu, V. (2001): Electro-mechanical impedance method for crack detection in thin plates, *Journal of Intelligent Material Systems and Structures*, vol. 12, pp. 709-718.

Zhou, S.W; Liang, C.A.; Rogers, C.A. (1995): Integration and Design of Piezoceramic Elements in Intelligent Structures, *Journal of Intelligent Materials Systems and Structures*, vol.6, pp. 733-743.